JBC RESEARCH ARTICLE

NOX4 regulates macrophage apoptosis resistance to induce fibrotic progression

Received for publication, February 15, 2021, and in revised form, May 3, 2021 Published, Papers in Press, May 21, 2021,
https://doi.org/10.1016/j.jbc.2021.100810

Jennifer L. Larson-Casey[1], Linlin Gu[1], Jungsoon Kang[1], Ashish Dhyani[1], and A. Brent Carter[1,2,*]

From the [1]Division of Pulmonary, Allergy, and Critical Care Medicine, Department of Medicine, University of Alabama at Birmingham, Birmingham, Alabama, USA; and [2]Birmingham Veterans Administration Medical Center, Birmingham, Alabama, USA

Edited by Dennis Voelker

Pulmonary fibrosis is a progressive lung disease often occurring secondary to environmental exposure. Asbestos exposure is an important environmental mediator of lung fibrosis and remains a significant cause of disease despite strict regulations to limit exposure. Lung macrophages play an integral role in the pathogenesis of fibrosis induced by asbestos (asbestosis), in part by generating reactive oxygen species (ROS) and promoting resistance to apoptosis. However, the mechanism by which macrophages acquire apoptosis resistance is not known. Here, we confirm that macrophages isolated from asbestosis subjects are resistant to apoptosis and show they are associated with enhanced mitochondrial content of NADPH oxidase 4 (NOX4), which generates mitochondrial ROS generation. Similar results were seen in chrysotile-exposed WT mice, while macrophages from *Nox4*$^{-/-}$ mice showed increased apoptosis. NOX4 regulated apoptosis resistance by activating Akt1-mediated Bcl-2-associated death phosphorylation. Demonstrating the importance of NOX4-mediated apoptosis resistance in fibrotic remodeling, mice harboring a conditional deletion of *Nox4* in monocyte-derived macrophages exhibited increased apoptosis and were protected from pulmonary fibrosis. Moreover, resolution occurred when *Nox4* was deleted in monocyte-derived macrophages in mice with established fibrosis. These observations suggest that NOX4 regulates apoptosis resistance in monocyte-derived macrophages and contributes to the pathogenesis of pulmonary fibrosis. Targeting NOX4-mediated apoptosis resistance in monocyte-derived macrophages may provide a novel therapeutic target to protect against the development and/or progression of pulmonary fibrosis.

The development of pulmonary fibrosis is a complex process leading to progressive collagen deposition in an aberrant manner. Asbestosis, the most debilitating type of asbestos-induced lung disease, remains to be an important cause of pulmonary fibrosis. Although strict regulatory controls exist to limit exposure, more than 1.3 million workers in the United States are exposed to hazardous levels of asbestos annually (1, 2). This results in more than 100,000 deaths annually in the United States (1, 2), and the incidence of asbestosis is increasing (3). There is no current treatment for asbestos-induced toxicity, including asbestosis, and recently approved antifibrotic therapies have limited efficacy (4, 5).

Lung macrophages play an integral role in the pathogenesis of asbestosis by initiating an immune response and generating reactive oxygen species (ROS), particularly mitochondrial ROS (6–8). Heterogeneity exists in the population of lung macrophages during fibrosis. In particular, monocyte-derived macrophages have recently been identified to be the critical myeloid cell in lung fibrosis (9–12). We and others have established that the predominance of a profibrotic monocyte-derived macrophage in the lung mediates progression of fibrotic repair (9, 11, 12), and the induction of phenotypic switching to an antifibrotic, or proinflammatory, phenotype halts further progression (11, 13–17).

Cellular death is critical for maintaining tissue homeostasis by eliminating damaged or genetically defective cells. Within the fibrotic lung, type II alveolar epithelial cells (AEC) undergo apoptosis in response to noxious stimuli. The expression of proapoptotic proteins is increased in AECs from subjects with pulmonary fibrosis, while a corresponding decrease is seen in antiapoptotic proteins (18). In contrast, myofibroblasts within fibroblastic foci in fibrotic lungs acquire an apoptosis-resistant phenotype that prevents resolution (19). Lung macrophages from subjects with idiopathic pulmonary fibrosis (IPF) exhibit apoptosis resistance with reduced caspase-3 cleavage (17); however, the mechanism by which this occurs has not been determined.

NADPH oxidase 4 (NOX4) is a constitutively active enzyme whose primary functions is to generate ROS, particularly hydrogen peroxide (20). NOX4 has been shown to be highly expressed in AECs from IPF subjects, and NOX4-mediated ROS generated by AECs has been implicated in inducing the apoptosis seen in these cells (21). *Nox4* has been reported to mediate the apoptosis resistance of IPF lung fibroblasts by inhibiting the transcription factor, nuclear factor erythroid-derived 2-like 2 (Nrf2), promoting redox imbalance, and myofibroblast senescence (19, 22). Recent data shows that apoptosis resistance occurs in fibrotic lung macrophages (17). We recently showed that NOX4 is crucial for lung macrophage profibrotic polarization to mediate fibrotic repair after asbestos

* For correspondence: A. Brent Carter, bcarter1@uab.edu.

exposure (11), but it is not known if NOX4 regulates apoptosis resistance in lung macrophages or if macrophage NOX4 is required for the progression of fibrotic repair.

Results

Mitochondrial NOX4 expression is associated with lung macrophage apoptosis resistance

To understand the role of apoptosis resistance in lung macrophages, we isolated lung macrophages from normal and asbestosis subjects. Normal subjects showed an increase in TUNEL positive cells compared with lung macrophages isolated from asbestosis subjects (Fig. 1*A*). Lung macrophages from asbestosis subjects showed significantly reduced caspase-3 activity compared with normal subjects (Fig. 1*B*). Because NOX4 is crucial for lung macrophage profibrotic polarization and profibrotic macrophages are associated with disease progression due to their prolonged survival (11, 12, 17, 23), we determined if NOX4 was expressed in lung macrophage mitochondria from subjects with asbestosis. NOX4 was increased 14-fold in the mitochondria from lung macrophages isolated from asbestosis subjects compared with normal

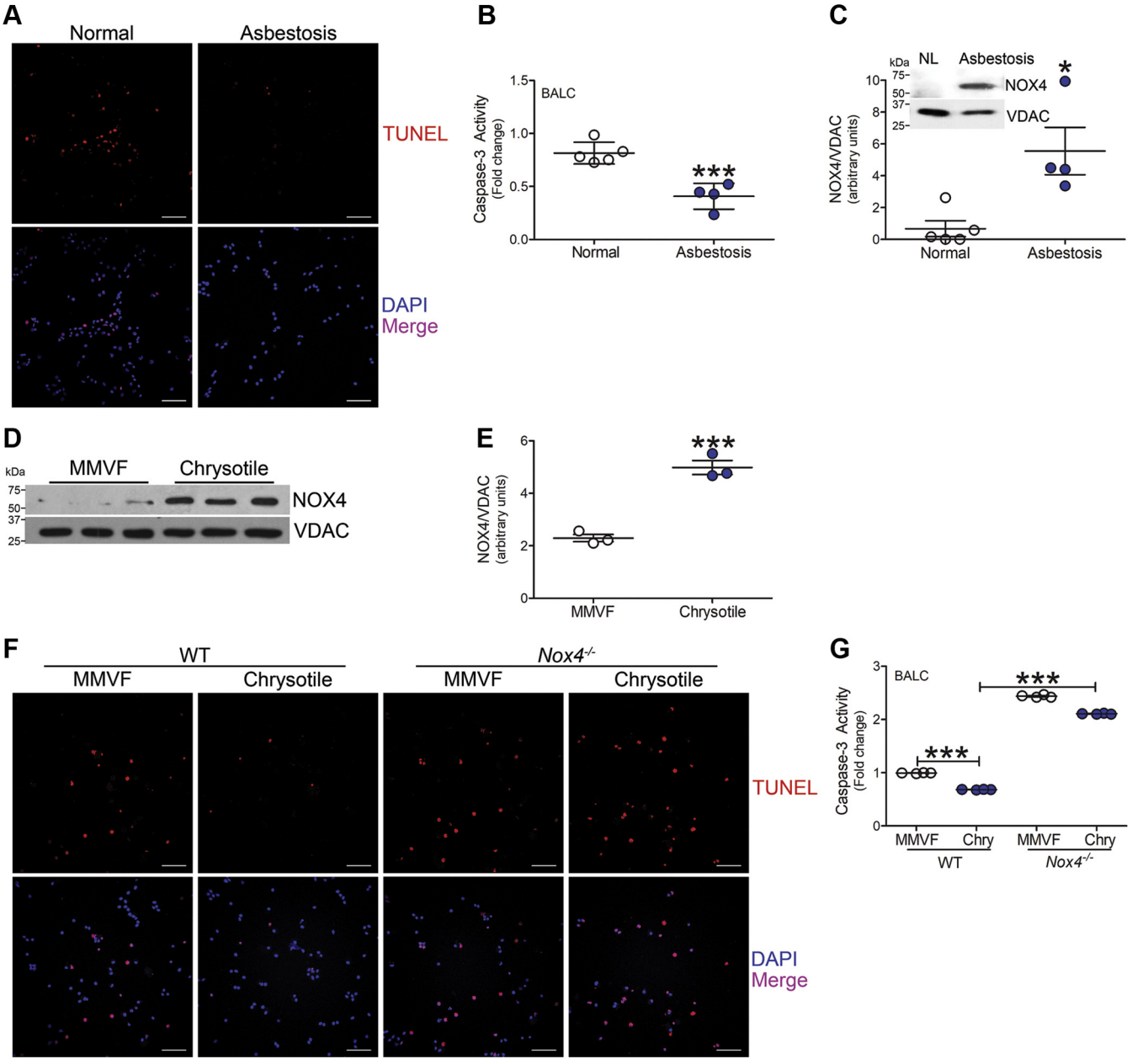

Figure 1. Mitochondrial NOX4 expression is associated with lung macrophage apoptosis resistance. BAL was performed on normal (n = 5) and asbestosis (n = 4) subjects. *A*, TUNEL staining, *B*, caspase-3 activity, *C*, quantification of NOX4 immunoblot analysis (*inset*). Mice were exposed to MMVF or chrysotile asbestos and were euthanized 21 days later. *D*, immunoblot analysis in mitochondrial fraction and *E*, quantification of immunoblot in *D* in WT mice (n = 3). *F*, TUNEL staining, and *G*, caspase-3 activity in WT (n = 4) and *Nox4*$^{-/-}$ mice (n = 4). Bar in *A* and *G* = 100 μm. *$p < 0.05$; ***$p < 0.0001$. Values shown as mean ± SEM. Two-tailed *t*-test statistical analysis was utilized for *B*, *C*, and *E*. One-way ANOVA followed by Tukey's multiple comparison test was utilized for *G*.

subjects (Fig. 1*C*). Similarly, mitochondrial NOX4 expression was significantly increased in WT mice with asbestos-induced lung fibrosis (Fig. 1, *D* and *E*).

To more directly link NOX4 to apoptosis resistance, chrysotile-exposed WT mice revealed a lack of TUNEL staining, while there was increased TUNEL staining in macrophages from *Nox4*$^{-/-}$ mice exposed to MMVF and chrysotile (Fig. 1*F*). Lung macrophages from chrysotile-exposed WT mice had decreased caspase-3 activity, whereas caspase-3 activity was increased in *Nox4*$^{-/-}$ mice (Fig. 1*G*). These data demonstrate that NOX4 has a critical role in mediating apoptosis resistance in lung macrophages.

Mice harboring a conditional deletion of Nox4 in monocyte-derived macrophages are protected from pulmonary fibrosis

To understand the role of monocyte-derived macrophages (MDMs) in fibrosis development, mice were exposed to chrysotile for 0, 5, 10, 15, and 21 days. Increased recruitment of MDMs and a reduction of resident alveolar macrophages (RAMs) were evident in mice 10 days after chrysotile exposure (Fig. 2, *A*–*C* and S1*A*). The number of RAMs decreased, while MDMs increased in a time-dependent manner. Similarly, CCL2 levels in the BAL fluid were significantly increased in 10 days after exposure to chrysotile with maximal levels seen at day 21 (Fig. 2*D*).

The conditional deletion of *Nox4* in macrophages (*Nox4*$^{-/-}$*Lyz2-cre*) abrogated the increase in MDMs after chrysotile exposure, and RAMs remained increased similar to the level seen in the MMVF control (Fig. 2, *E*–*G*). BAL fluid from *Nox4*$^{-/-}$*Lyz2-cre* mice showed significantly reduced CCL2 levels, suggesting a potential mechanism for the reduced MDM recruitment in the chrysotile-exposed mice (Fig. 2*H*).

We questioned which monocyte/macrophage cell subset had NOX4-mediated apoptosis resistance during fibrosis. RAMs from chrysotile-exposed WT mice displayed apoptosis resistance, while *Nox4*$^{-/-}$*Lyz2-cre* RAMs showed significantly greater caspase-3 activity (Fig. 2*I*). Chrysotile exposure significantly reduced caspase-3 activity in MDMs from WT mice, and *Nox4*$^{-/-}$*Lyz2-cre* MDMs showed activity similar to WT controls (Fig. 2*J*). The absence of NOX4-mediated apoptosis resistance in MDMs protected *Nox4*$^{-/-}$*Lyz2-cre* mice from pulmonary fibrosis (Fig. S1*B*). In contrast, the Masson's trichrome staining showed dense collagen deposition in chrysotile-exposed WT mice. The histological findings were confirmed biochemically by hydroxyproline assay (Fig. S1*C*). These observations suggest that NOX4 expression in MDMs mediates apoptosis resistance that has a critical role in fibrotic repair.

NOX4 mediates apoptosis resistance via *phosphorylation of BAD*

To determine the mechanism by which NOX4 mediates apoptosis resistance, we focused on downstream signaling of NOX4. We determined if Akt1 is modulated by NOX4 in lung macrophages. The mitochondrial localization of NOX4 was induced in macrophages treated with chrysotile asbestos or in macrophages expressing NOX4. The combination increased expression further (Fig. 3*A*). NOX4 expression correlated with Akt1 activation, as chrysotile exposure and NOX4 expression induced the activation of Akt1. The opposite was seen in macrophages with NOX4 silenced, and there was no effect with chrysotile exposure (Fig. 3*B*). Likewise, bone-marrow-derived macrophages (BMDM) isolated from *Nox4*$^{-/-}$ mice showed an absence of Akt1 activation (Fig. 2*C*).

Because NOX4 overexpression diminishes caspase-3 activity in macrophages (Fig. 3*D*), we questioned if this was mediated in an Akt-dependent manner. Overexpression of NOX4 induced Akt1 activation and Bcl-2-associated death (BAD) phosphorylation at Ser^{136} (Fig. 3*E*). BAD phosphorylation was mediated by Akt1 as silencing *Akt1* in macrophages expressing NOX4 showed an absence of BAD phosphorylation. Unphosphorylated BAD increased caspase-3 activity in macrophages with *Akt1* silenced (Fig. 3*F*). Further demonstrating these effects were mediated by Akt1 activation, *Nox4* silencing inhibited Akt1 activation and BAD phosphorylation (Fig. 3*G*); however, macrophages expressing constitutively active Akt1 with *Nox4* silenced led to Akt1 activation and phosphorylation of BAD. Akt1-mediated phosphorylation of BAD inhibited caspase-3 activity (Fig. 3*H*). Implicating the importance of Akt1 activation, we showed that phosphatase and tensin homologue (PTEN) expression was reduced in chrysotile-exposed macrophages (Fig. S2). Moreover, phosphorylation of apoptosis signal-regulating kinase 1 (ASK1) was similarly reduced.

Validating that NOX4 mediated apoptosis resistance *via* BAD phosphorylation, we found that the proapoptotic proteins, Bax and Bak, had cytoplasmic localization in macrophages expressing NOX4 or exposed to chrysotile (Fig. 3*I*). To confirm the relationship of BAD to resistance of apoptosis, NOX4 mediated activation of Akt1 in macrophages with *Bad* silenced (Fig. 3*J*), and the absence of BAD expression reduced caspase-3 activity (Fig. 3*K*).

To determine the biological relevance of BAD *in vivo*, the absence of NOX4 in MDMs from *Nox4*$^{-/-}$*Lyz2-cre* mice was associated with absent Akt1 activation and BAD phosphorylation, whereas chrysotile-exposed WT mice showed increased Akt1 activation and BAD phosphorylation (Fig. 3L). In humans, asbestosis subjects showed increased NOX4 and activation of Akt1, which correlated with a significant increase in BAD phosphorylation in lung macrophages compared with normal volunteers (Fig. 3, *M*–*P*). These data strongly suggest that NOX4 mediates apoptosis resistance *via* phosphorylation of BAD in an Akt1-dependent manner.

NOX4-mediated mitochondrial ROS is required for apoptosis resistance

Because mtROS in lung macrophages is linked to fibrotic repair (6–8, 17), we measured ROS generation in macrophages from chrysotile-exposed mice. WT mice exposed to chrysotile had increased H_2O_2 generation in the lung macrophages, whereas the H_2O_2 generation in macrophages from chrysotile-exposed *Nox4*$^{-/-}$ mice was below control levels (Fig. 4*A*).

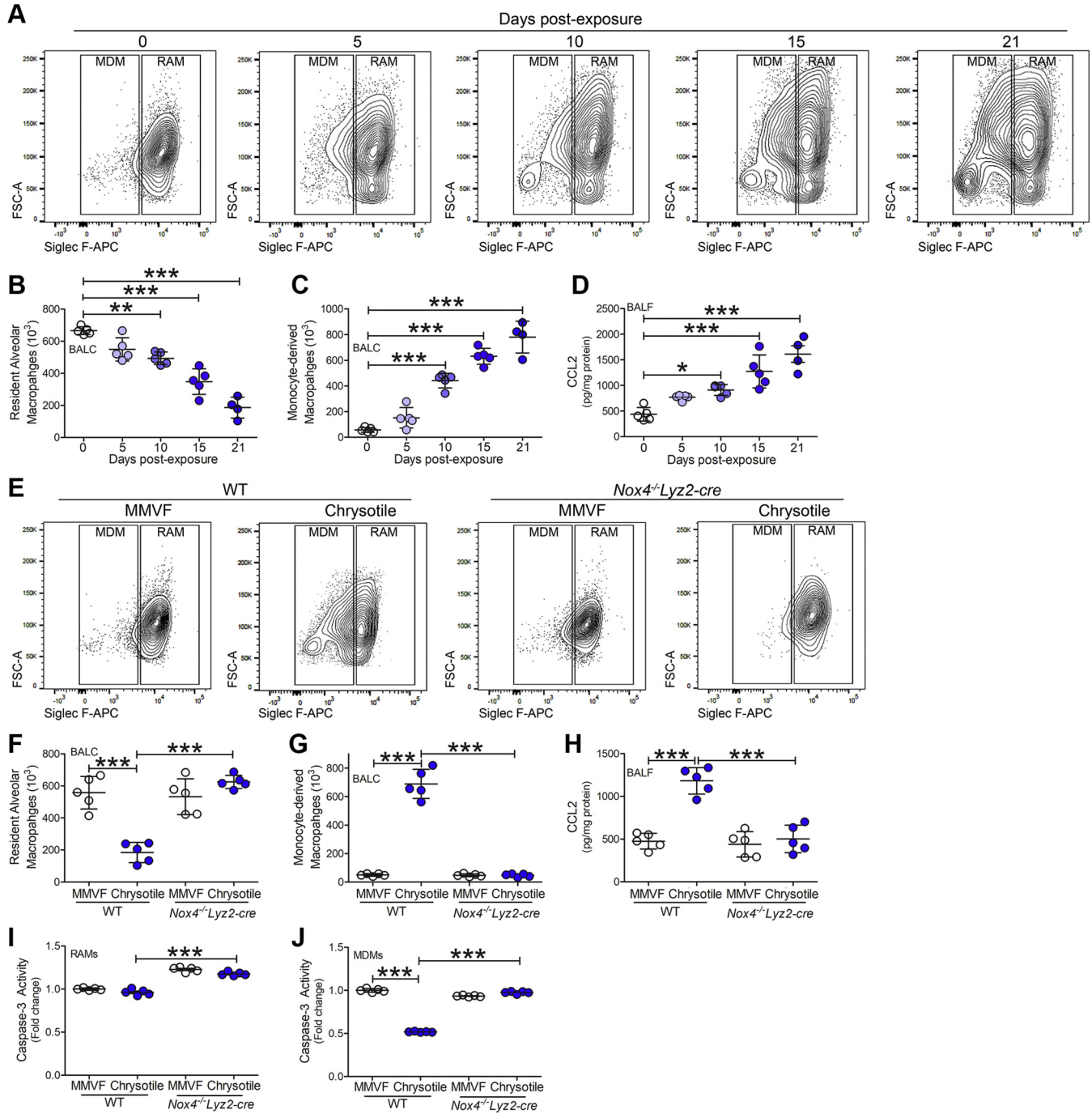

Figure 2. Mice harboring a conditional deletion of *Nox4* in monocyte-derived macrophages are protected from pulmonary fibrosis. WT mice were exposed to chrysotile and BAL was harvested on day 0, 5, 10, 15, and 21. *A*, representative flow cytometry plots of resident alveolar macrophages (RAM, $CD45^+CD11b^{+/-}Ly6G^-CD64^+Ly6c^-Siglec\ F^{hi}$) and monocyte-derived macrophages (MDM, $CD45^+CD11b^{+/-}Ly6G^-CD64^+Ly6c^-Siglec\ F^{low}$). Number of flow sorted *B*, RAMs ($n = 4–5$) and *C*, MDMs ($n = 4–5$). *D*, CCL2 levels in BAL fluid ($n = 4–5$). WT and $Nox4^{-/-}Lyz2\text{-}cre$ mice were exposed to MMVF or chrysotile. BAL was performed on day 21. *E*, Representative flow cytometry plots of RAMs and MDMs. Number of flow sorted *F*, RAMs ($n = 5$) and *G*, MDMs ($n = 5$). *H*, CCL2 levels in BAL fluid ($n = 5$). *I*, Caspase-3 activity in RAMs ($n = 5$) and *J*, MDMs ($n = 5$). $^{**}p < 0.001$; $^{***}p < 0.0001$. Values shown as mean ± SEM. One-way ANOVA followed by Tukey's multiple comparison test was utilized.

Confirming that mtROS generation regulated NOX4-mediated apoptosis resistance, we isolated BMDM from WT and $Nox4^{-/-}$ mice. MitoTEMPO reduced mtROS generation from chrysotile-exposed BMDM from WT mice to control levels, and mtROS generation from $Nox4^{-/-}$ BMDM showed greater reduction regardless of treatment (Fig. 4*B*). MitoTEMPO treatment reduced NOX4 expression, Akt1 activation, and BAD phosphorylation in chrysotile-exposed BMDM from WT mice, whereas NOX4, activated Akt1, and phosphorylated BAD were essentially absent in $Nox4^{-/-}$ BMDM (Fig. 4*C*). NOX4-meditaed mtROS generation led to a significant reduction in caspase-3 activity in WT BMDM, and

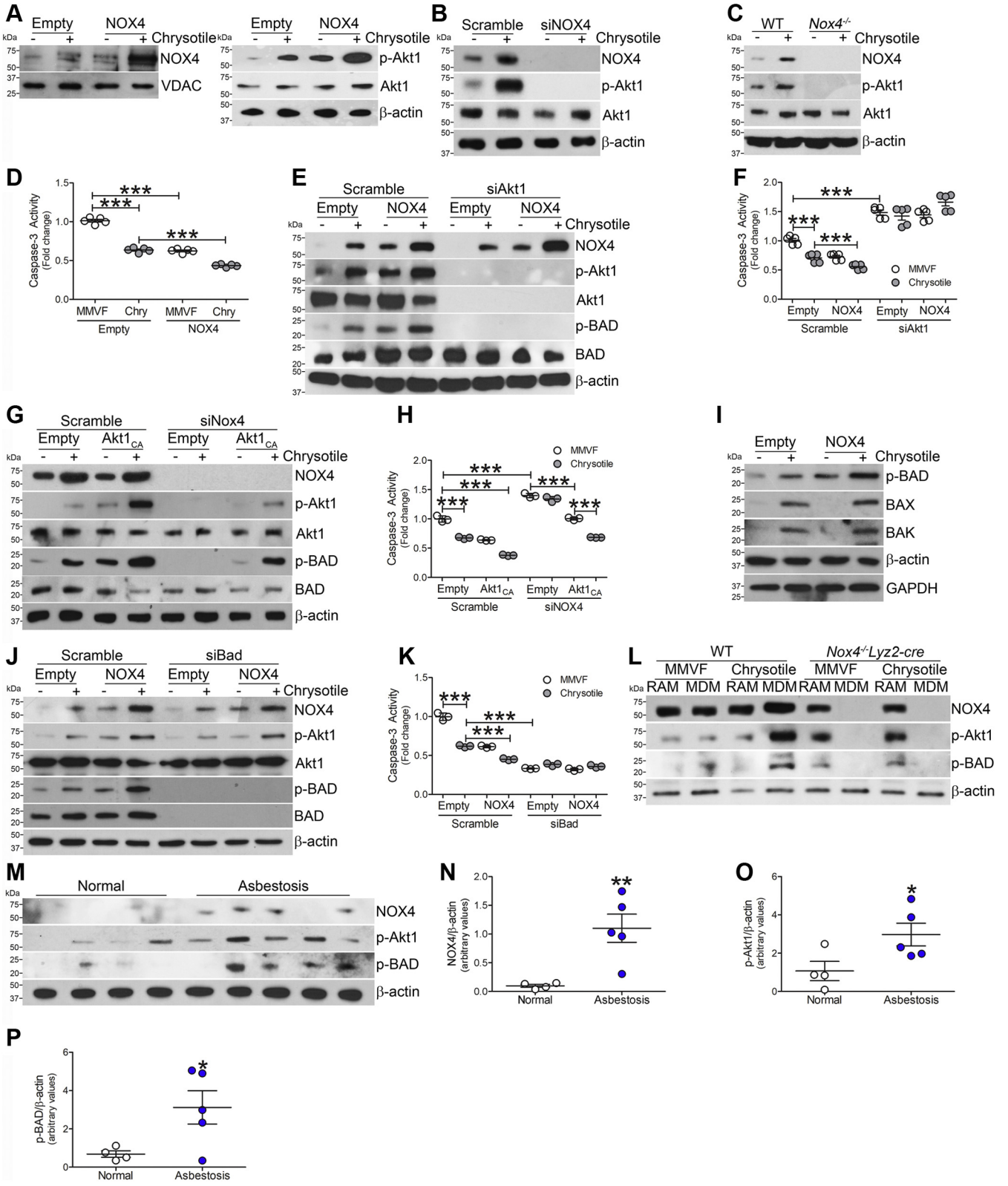

Figure 3. NOX4 mediates apoptosis resistance *via* phosphorylation of BAD. *A*, immunoblot analysis of macrophages (THP-1 cells) expressing empty or NOX4 exposed to chrysotile. *B*, immunoblot analysis of macrophages (THP-1 cells) transfected with scramble or NOX4 siRNA. *C*, immunoblot analysis of bone-marrow-derived macrophages isolated from WT and *Nox4*$^{-/-}$ mice and exposed to MMVF or chrysotile. *D*, Caspase-3 activity in macrophages (THP-1 cells) expressing empty or NOX4 treated with chrysotile (n = 5). Macrophages (THP-1 cells) expressing empty or NOX4 were transfected with scramble or Akt1 siRNA. *E*, immunoblot analysis and *F*, caspase-3 activity (n = 5). *G*, immunoblot analysis and *H*, caspase-3 activity of macrophages (THP-1 cells) expressing empty or $Akt1_{CA}$ that were transfected with scramble or NOX4 siRNA. *I*, immunoblot analysis of macrophages expressing empty or NOX4 treated with chrysotile. Macrophages (MH-S cells) expressing empty or NOX4 were transfected with scramble or *Bad* siRNA. *J*, immunoblot analysis and *K*, caspase-3 activity (n = 3). *L*, representative immunoblot analysis from flow sorted RAMs (n = 5) and MDMs (n = 5) from WT and *Nox4*$^{-/-}$*Lyz2-cre* mice were exposed to

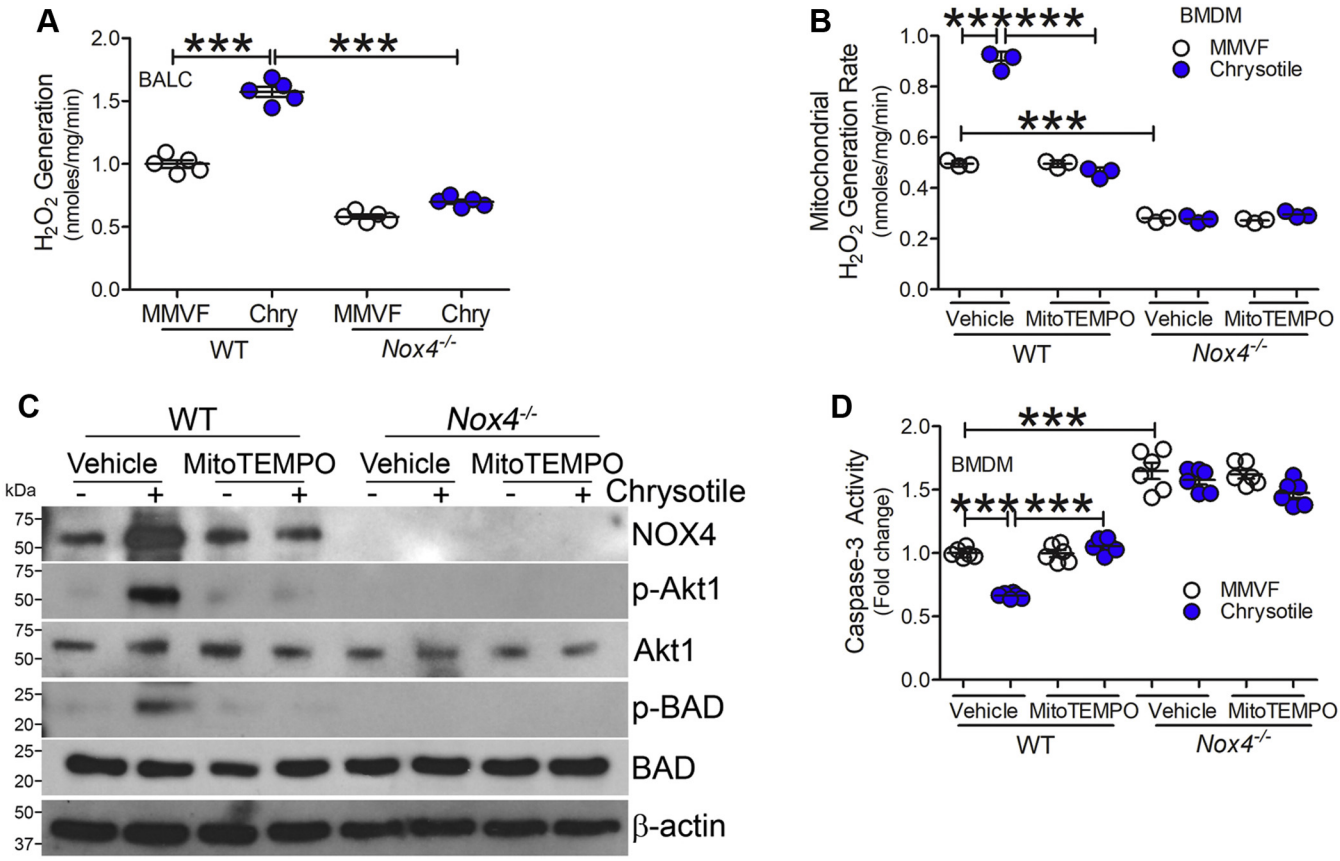

Figure 4. NOX4-mediated mitochondrial ROS is required for apoptosis resistance. *A*, H_2O_2 generation was measured in BAL cells isolated from WT (n = 5) and *Nox4*$^{-/-}$ (n = 5) mice were exposed to MMVF or chrysotile. Bone-marrow-derived macrophages were isolated from WT and *Nox4*$^{-/-}$ mice and treated with vehicle or mitoTEMPO (10 μM, 16 h) and MMVF or chrysotile. *B*, Mitochondrial H_2O_2 (n = 3), *C*, immunoblot analysis, and *D*, caspase-3 activity (n = 6) were measured. ***$p < 0.0001$. Values shown as mean ± SEM. One-way ANOVA followed by Tukey's multiple comparison test was utilized.

MitoTEMPO treatment increased caspase-3 activity to control levels (Fig. 4*D*). BMDM from *Nox4*$^{-/-}$ mice showed increased caspase-3 activity compared with WT, and neither chrysotile nor MitoTEMPO altered the activity. These data suggested that macrophage NOX4 modulated apoptosis resistance by regulating mtROS to mediate Akt1 phosphorylation of BAD at Ser^{136}.

Macrophage Nox4 regulates progression of dysregulated fibrotic repair

To determine the role of macrophage NOX4 in apoptosis resistance during progression of fibrotic remodeling, *Nox4* was conditionally deleted in mice after fibrosis was established. Mice harboring a conditional deletion of *Nox4* in MDMs were generated using a tamoxifen-inducible Cre driven by the colony-stimulating factor 1 receptor (Csf1r) promoter (*Nox4*$^{-/-}$*Csf1r*^{MeriCreMer}). We verified that fibrosis was evident in *Nox4*$^{fl/fl}$ and *Nox4*$^{-/-}$*Csf1r*^{MeriCreMer} mice 12 days after exposure to chrysotile (Fig. 5, *A* and *B*). In subsequent experiments, tamoxifen was administered to MMVF- and chrysotile-exposed *Nox4*$^{fl/fl}$ and *Nox4*$^{-/-}$*Csf1r*^{MeriCreMer} mice starting at day 12. Chrysotile-exposed *Nox4*$^{fl/fl}$ mice had a reduction in the number of RAMs compared with MMVF-exposed *Nox4*$^{fl/fl}$ and *Nox4*$^{-/-}$*Csf1r*^{MeriCreMer} mice (Fig. 5, *C* and *D*). The reduction of RAMs was associated with a significant increase of MDMs in chrysotile-exposed *Nox4*$^{fl/fl}$ mice, while *Nox4*$^{-/-}$*Csf1r*^{MeriCreMer} mice showed an absence of MDM recruitment (Fig. 5, *C* and *E*).

Tamoxifen administration depleted NOX4 expression in FACS-sorted MDMs from *Nox4*$^{-/-}$*Csf1r*^{MeriCreMer} mice, while RAMs retained NOX4 expression (Fig. 5*F*). Chrysotile-exposed *Nox4*$^{fl/fl}$ mice administered tamoxifen showed an increase of NOX4 in MDMs compared with RAMs. The absence of NOX4 in MDMs from *Nox4*$^{-/-}$*Csf1r*^{MeriCreMer} mice resulted in an absence in Akt1 activation and phosphorylation of BAD. There was no significant difference in caspase-3 activity in RAMs from *Nox4*$^{fl/fl}$ mice and *Nox4*$^{-/-}$*Csf1r*^{MeriCreMer} mice (Fig. 5*G*). MDMs showed a significant decrease in caspase-3 activity in chrysotile-exposed *Nox4*$^{fl/fl}$ mice, whereas it was significantly increased in *Nox4*$^{-/-}$*Csf1r*^{MeriCreMer} mice (Fig. 5*H*).

To determine the impact of NOX4 regulating lung macrophage profibrotic polarization, we analyzed profibrotic

MMVF or chrysotile. BAL was performed on normal (n = 4) and asbestosis (n = 5) subjects. *M*, immunoblot analysis, quantification of *N*, NOX4, *O*, p-Akt1, and *P*, p-BAD immunoblots in *M* were conducted. *$p < 0.05$; **$p < 0.001$; ***$p < 0.0001$. Values shown as mean ± SEM. Two-tailed *t*-test statistical analysis was utilized for *N-P*. One-way ANOVA followed by Tukey's multiple comparison test was utilized for *D*, *F*, *H*, *K*.

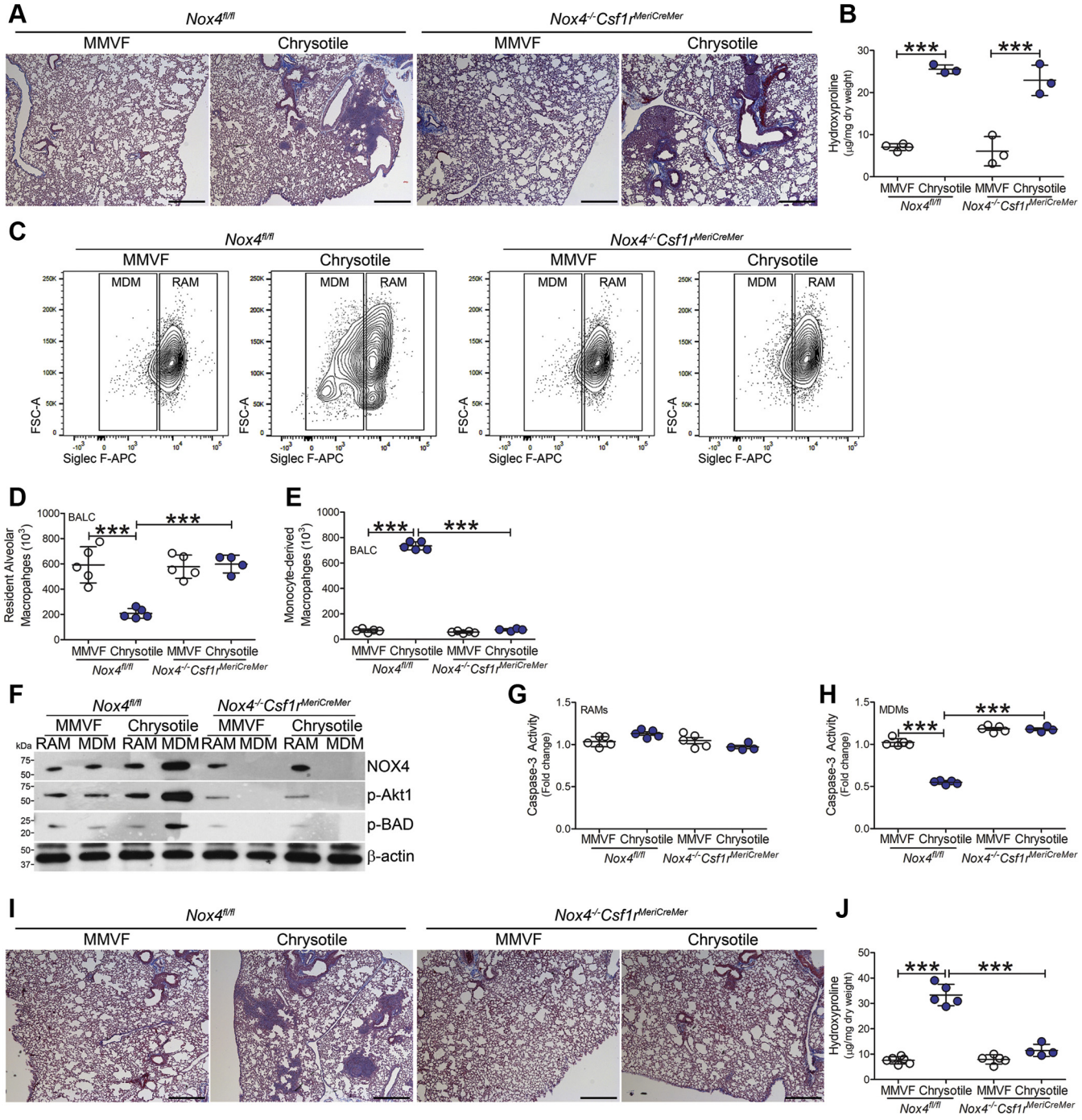

Figure 5. Macrophage Nox4 regulates progression of dysregulated fibrotic repair. *Nox4*$^{fl/fl}$ and *Nox4*$^{-/-}$*Csf1r*^{MeriCreMer} mice were harvested 12 days exposure to MMVF or chrysotile. *A*, representative histology of lung sections with Masson's trichrome staining (n = 3) and *B*, hydroxyproline analysis of homogenized lung (n = 3). *Nox4*$^{fl/fl}$ and *Nox4*$^{-/-}$*Csf1r*^{MeriCreMer} mice were exposed to MMVF or chrysotile. Mice were subjected to tamoxifen injections (75 mg/kg, i.p. daily) for 5 consecutive days beginning at day 12. BAL was performed on day 21. *C*, representative flow cytometry plots of RAMs and MDMs. Number of flow sorted *D*, RAMs (n = 4–5) and *E*, MDMs (n = 4–5). *F*, immunoblot analysis and caspase-3 activity in *G*, RAMs (n = 4–5) and *H*, MDMs (n = 4–5). *I*, representative histology of lung sections with Masson's trichrome staining (n = 4–5) and *J*, hydroxyproline analysis of homogenized lung (n = 4–5). ***$p <$ 0.0001. Bar = 500 µm in *A* and *I*. Values shown as mean ± SEM. Two-tailed *t*-test statistical analysis was utilized for *B*. One-way ANOVA followed by Tukey's multiple comparison test was utilized for *D-E*, *G-H*, *J*.

cytokines in BAL fluid from *Nox4*$^{fl/fl}$ and *Nox4*$^{-/-}$ *Csf1r*^{MeriCreMer} mice. BAL fluid isolated 12 days after chrysotile exposure (prior to tamoxifen injection) showed increased PDGF-BB and IL-10 levels in BAL fluid from both strains (Fig. S3, *A* and *B*). Tamoxifen-induced deletion of *Nox4* reduced PDGF-BB and IL-10 levels near control levels, while *Nox4*$^{fl/fl}$ mice showed a further increase 21 days after chrysotile exposure. We then determined if NOX4 regulates lung macrophage profibrotic polarization *via* Akt1-mediated BAD phosphorylation. Arginase activity was increased in

macrophages expressing NOX4, and exposure to chrysotile increased the activity further (Fig. S3*C*). The silencing of Bad in macrophages significantly reduced arginase activity below control levels, implicating the importance of this pathway in the regulation of profibrotic polarization.

The deletion of *Nox4* mediated resolution in established fibrosis. MMVF-exposed $Nox4^{fl/fl}$ and $Nox4^{-/-}Csf1r^{MeriCreMer}$ mice showed normal lung architecture. Chrysotile-exposed $Nox4^{-/-}Csf1r^{MeriCreMer}$ showed resolution of collagen deposition in the lungs compared with architectural distortion in the chrysotile-injured $Nox4^{fl/fl}$ mice (Fig. 5*I*). Tamoxifen-induced deletion of *Nox4* in $Nox4^{-/-}Csf1r^{MeriCreMer}$ mice with established fibrosis led to significantly reduced hydroxyproline content to the level seen in the MMVF-exposed $Nox4^{fl/fl}$ mice (Fig. 5*J*). These results demonstrated that NOX4 regulated MDM apoptosis resistance and reversed fibrotic remodeling. These observations suggest that targeting macrophage NOX4 in pulmonary fibrosis may reverse disease progression.

Discussion

NOX4 has been implicated in many fibrotic diseases, including the skin (24), liver (25), pancreas (26), kidney (27), heart (28), and lung (11, 19, 21). Within the lung, NOX4 has been shown to be increased in myofibroblasts, alveolar epithelial cells, and macrophages to promote the development of pulmonary fibrosis. Studies showed TGF-β1 regulates NOX4 expression in IPF lung fibroblasts to mediate mtROS production (29). NOX4 modulates myofibroblast activation by regulating Nrf2 to influence fibroblast apoptosis resistance (19). Similarly, AECs stimulated with TGF-β1 showed increased NOX4 expression to regulate ROS generation (21). NOX4-dependent ROS was necessary for TGF-β1-induced AEC injury and apoptosis. We showed that NOX4 is crucial for lung macrophage profibrotic polarization and fibrotic remodeling (11). $Nox4^{-/-}$ macrophages failed to polarize to the profibrotic phenotype and had reduced mtROS production. Contrary to fibroblasts and AECs, NOX4 regulated TGF-β1 expression in macrophages by mediating mtROS. Here we show that NOX4 regulates apoptosis resistance in macrophages by a redox-dependent mechanism.

During fibrotic remodeling in the lung, AECs often undergo apoptosis. Studies show that activation of the Fas-Fas ligand pathway in AECs promoted pulmonary fibrosis (30). Apoptotic, hyperplastic epithelial cells are present in IPF subjects and exhibit caspase-3 activation and inhibition of Bcl-2 (18). ER stress in AECs has been shown to predispose the lung to fibrotic remodeling in experimental models (31). IPF fibroblasts exhibit apoptosis resistance *via* increased expression of Bcl-2 (32), while other studies indicate that IPF fibroblasts are also resistant to Fas-mediated apoptosis (33). The role of apoptosis in macrophages has been controversial. Bleomycin has been shown to induce apoptosis in alveolar macrophages treated *ex vivo* (34). Administration of apoptotic macrophages in the lungs of rats promoted macrophage infiltration and apoptosis, impaired efferocytosis, and induced development of pulmonary fibrosis (35). Recent data implicated that apoptosis resistance occurs in lung macrophages and is associated to the profibrotic polarization of macrophages (17). IPF lung macrophages require mitophagy for the removal of dysfunctional mitochondria, which induces apoptosis resistance. Implicating the importance of macrophages in fibrosis, several studies demonstrated that promoting apoptosis of recruited lung macrophages protects mice from lung fibrosis (9, 10). Here we show that NOX4 mediates apoptosis resistance in MDMs by regulating BAD in a redox-dependent manner (Fig. 6). Apoptosis resistance in RAMs does not require BAD phosphorylation, supporting the notion that RAMs do not contribute to fibrosis. We cannot rule out that apoptosis in RAMs may occur *via* other proteins or signaling pathways, as NOX4 has been shown to alter Bcl-2 expression (36). Moreover, modulating NOX4-mediated macrophage apoptosis in established fibrosis results in the resolution of asbestos-induced pulmonary fibrosis.

NOX4 has been shown to regulate Akt activation in the kidney, vasculature, and heart (37–39). Akt, also known as protein kinase B (PKB), is a serine/threonine protein kinase mediating cell growth, metabolism, and ROS production. The prosurvival signaling by Akt is associated with many human cancers, diabetes, neurodegenerative disorders, and Akt is upregulated in various fibrotic tissues (40–43). Within the fibrotic lung, Akt has been shown to be increased in IPF fibroblasts (44), and single-cell RNA sequencing has identified Akt activation in IPF epithelial cells, including basal cells (45). While we have shown that Akt1 is activated in lung macrophages from subjects with IPF (17), NOX4 has not previously been connected to the regulation of Akt1 activation in humans with pulmonary fibrosis.

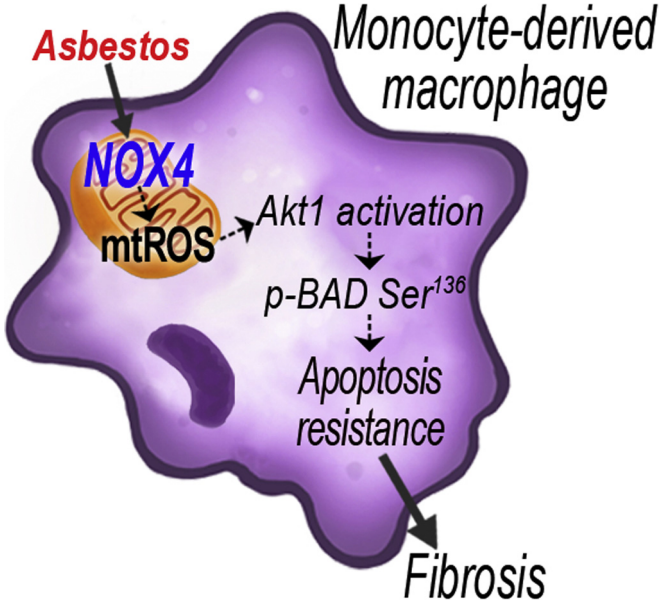

Figure 6. Macrophage Nox4 regulates fibrotic progression in monocyte-derived macrophages. Asbestos exposure promotes the mitochondrial localization of NOX4, which mediates mitochondrial ROS (mtROS) to activate Akt1. The phosphorylation of BAD at Ser^{136} by Akt1 mediated apoptosis resistance in monocyte-derived macrophages and increased fibrotic remodeling.

BAD regulates apoptosis by interacting with Bcl-2 and Bcl-X_L (46). While Bcl-2 and Bcl-X_L promote apoptosis resistance by binding to Bax and preventing the release of cytochrome *c* from the mitochondria, the binding of BAD with Bcl-2 or Bcl-X_L sequesters these proteins in the cytoplasm to induce apoptosis. Akt specifically phosphorylates BAD on serine[136] (equivalent of the human serine 99 residue) leading to the inability of BAD to heterodimerize with Bcl-2 or Bcl-X_L (47), thus permitting them to bind to Bax to block apoptosis.

While mtROS is linked to apoptosis and apoptosis resistance, the relationship of NOX4 and apoptosis in macrophages is not known. Our studies show that NOX4-mediated apoptosis resistance in monocyte-derived macrophages was redox-dependent. Our results contrast those found in cardiac myocytes, where ROS induced the translocation of BAD to the mitochondria and its binding with Bcl-2 to provoke apoptosis (47). Our data indicated that deletion of macrophage *Nox4* in mice with established fibrosis induced resolution of the disease. Moreover, these observations provide a mechanism by which NOX4 regulates apoptosis resistance in MDMs to promote progression of fibrosis and suggest a novel therapeutic target to prevent ongoing aberrant fibrotic remodeling.

Experimental procedures

Human subjects

Human BAL cells were obtained as previously described (8) from normal subjects and asbestosis patients under an approved protocol by the Human Subjects Institutional Review Board of UAB (300001124) and the Birmingham VAMC (01670). These studies abide by the Declaration of Helsinki principles. Human BAL specimens were used for research only. All subjects provided prior written consent to participate in the study. Normal volunteers had to meet the following criteria: (1) age between 18 and 65 years; (2) no history of cardiopulmonary disease or other chronic disease; (3) no prescription or nonprescription medication except oral contraceptives; (4) no recent or current evidence of infection; and (5) lifetime nonsmoker. Asbestosis subjects had to meet the following criteria: (1) FVC (forced vital capacity) at least 50% predicted; (2) current nonsmoker; (3) no recent or current evidence of infection; (4) evidence of restrictive physiology on pulmonary function tests; and (5) usual interstitial pneumonia on high-resolution chest computed tomography. Fiberoptic bronchoscopy with bronchoalveolar lavage was performed after subjects received local anesthesia. Three subsegments of the lung were lavaged with five 20-ml aliquots of normal saline, and the first aliquot in each was discarded. The percentage of macrophages was determined by Wright–Giemsa stain and varied from 90 to 98%.

Mice

Animal experiments were approved by UAB Institutional Animal Care and Use Committee (21149) and were performed in accordance with NIH guidelines. Eight- to twelve-week-old male and female mice were intratracheally administered 100 μg of chrysotile asbestos or man-made vitreous fiber (MMVF), as a negative control, after being anesthetized with 3% isoflurane using a precision Fortec vaporizer. BAL was performed 21 days after exposure. WT C57BL6 mice were purchased from JAX Labs, *Nox4*$^{-/-}$ have been previously described (21), and *Nox4*$^{-/-}$*Lyz2-cre* were generated by selective disruption of *Nox4* gene in lineage cells of the granulocyte/monocyte lineage by crossing *Nox4*$^{fl/fl}$ mice with mice containing a Cre recombinase under control of the lysozyme M promoter as previously described (11). *Nox4*$^{-/-}$*Csf1r*^{MeriCreMer} mice were generated by crossing *Nox4*$^{fl/fl}$ mice with tamoxifen inducible Mer-iCre-Mer driven by the *Csf1r* promoter (FVB-Tg(Csf1r-cre/Esr1*)1Jwp/J, stock number 019098, Jackson Laboratory). *Nox4* was selectively and conditionally deleted from the monocytes/macrophages by tamoxifen-containing food or following administration of tamoxifen (75 mg/kg, i.p.) 12 days after chrysotile or MMVF exposure and continued daily for 5 consecutive days.

Cell culture

Human monocyte (THP-1) and mouse alveolar macrophage (MH-S) cell lines were obtained from American Type Culture Collection. Cells were maintained in RPMI 1640 media with 10% fetal bovine serum and penicillin/streptomycin supplements. All experiments were conducted in RPMI containing 0.5% serum.

Plasmids, transfections, and small interfering RNA (siRNA)

The pcDNA3.1-NOX4 and pUSE-Akt1$_{CA}$ plasmids have been previously described (11, 23). Cells were transfected using X-treme GENE 9 Transfection Reagent (Sigma) according to the manufacturer's protocol. Cells were transfected with 100 nM scramble, human Akt1, human NOX4, or mouse Bad siRNA duplex (IDT) utilizing Dharmafect 2 (Thermo Scientific) according to manufacturer's protocol. Eight hours after transfection, media was replaced, and cells were allowed to recover for 24–72 h.

Flow cytometry

BAL cells were blocked with 1% BSA containing TruStain fcX (anti-mouse CD16/32) antibody (101319; BioLegend), followed by staining with antibodies. Antibodies used: Rat anti-mouse CD45-PE (12–0451–82; eBiosciences), LIVE Dead-eflour506 (65–0866; Invitrogen), Rat anti-mouse CD11b-APC-Cy7 (101225; BioLegend), anti-mouse CD64-PE-Cy7 (139313; BioLegend), Rat anti-mouse Ly6G-AF700 (561236; BD), Rat anti-mouse Siglec F-APC (155507; BioLegend), and Rat anti-mouse Ly6C: eflour450 (48–5932–82; Invitrogen). Hierarchical gating strategy was used to represent the resident alveolar macrophages as CD45$^+$CD11b$^{+/-}$Ly6G$^-$CD64$^+$Ly6c$^-$Siglec F^{hi} and monocyte-derived macrophages as CD45$^+$CD11b$^{+/-}$Ly6G$^-$CD64$^+$Ly6c$^-$ Siglec F^{low}. To determine cell number, CountBright Absolute Counting Beads (Molecular Probes) were added according to manufacturer's instructions. Briefly, counting beads were gently vortexed and 50 μl was added to stained cells in a volume of 300 μl. Counting beads were gated on forward

versus linear side scatter. The following equation was used to determine cell number: (number of cell events/number of bead events) × (lot specific bead count per 50 μl/volume of sample). Data was acquired on FACSAria II or LSR II (BD Biosciences) using BD FACS DIVA software (version 8.0.1). Data was analyzed using FlowJo (FlowJo LLC) software (Version 10.5.0).

Determination of H_2O_2 generation

H_2O_2 production was determined fluorometrically. Cells were incubated in phenol-red free Hanks' balanced salt solution supplemented with 6.5 mM glucose, 1 mM HEPES, 6 mM sodium bicarbonate, 1.6 mM pHPA, and 0.95 μg/ml HRP. Fluorescence of pHPA-dimer was measured using a spectrofluorometer at excitation of 320 nm and emission of 400 nm (17).

Isolation of mitochondria and cytoplasm

Mitochondria were isolated by lysing the cells in mitochondria buffer containing 10 mM Tris, pH 7.8, 0.2 mM EDTA, 320 mM sucrose, and protease inhibitors. Lysates were homogenized using a Kontes Pellet Pestle Motor and centrifuged at 2000*g* for 8 min at 4 °C. The supernatant was removed and incubated at 4 °C and the pellet was lysed, homogenized, and centrifuged again. The two supernatants were pooled and centrifuged at 12,000*g* for 15 min at 4 °C. The pellet was washed in the mitochondrial buffer twice and then resuspended in mitochondria buffer without sucrose (8).

Immunoblot analysis

Primary antibodies used: Akt1 (2938), Bad (9239), Lamin A/C (2032), Bax (2772), phospho-Akt1 (9018), phospho-Bad (Ser136) (4366), VDAC (4866) (Cell Signaling); β-actin (A5441) (Sigma); p38 (sc-7972) (Santa Cruz); NOX4 (NB110-58849) (Novus), NOX4 (109225) (Abcam); Bak (A0404) (Abclonal).

ELISA

CCL2 expression was determined in BALF using ELISA kits (R&D Systems) according to the manufacturer's instructions.

TUNEL assay

Detection of apoptosis was determined in BAL cells by TUNEL analysis, *in situ* Cell Death Detection Kit, TMR red (Sigma) according to the manufacturer's instructions and as previously described (23). BAL cells were fixed with 4% paraformaldehyde in PBS, permeabilized, and counterstained with DAPI. Nikon A1 Confocal was utilized for imaging.

Caspase-3 activity

Caspase-3 activity was measured using EnzChek Caspase-3 Assay Kit Number 2 (Molecular Probes) according to the manufacturer's protocol. Cells were lysed in 1 × lysis buffer, subjected to a freeze–thaw cycle, centrifuged to remove cellular debris, and loaded into individual microplate wells. The 2× reaction buffer with substrate was immediately added to the samples, and fluorescence was measured (excitation/emission 496/520 nm). Activity was normalized to protein concentration in each sample. A supplied inhibitor was used as a negative control in all experiments (23).

Hydroxyproline assay

Lung tissues were dried to a stable weight and acid hydrolyzed with 6N HCl for 24 h at 110 °C. Samples were resuspended in 1.5 ml phosphate-buffered saline followed by incubation at 60 °C for 1 h. Samples were centrifuged at 13,000 rpm, and the supernatant was taken for hydroxyproline analysis by using chloramine-T. Hydroxyproline concentration was normalized to the dry weight of the tissue (17).

Statistical analysis

Statistical comparisons were performed using a Student's *t*-test when only two groups of data are presented, or one-way ANOVA with a Tukey's *post hoc* test. All statistical analysis was expressed as ±SEM and $p < 0.05$ was considered to be significant. GraphPad Prism statistical software was used for all analysis.

Data availability

All data are contained within the article.

Supporting information—This article contains supporting information.

Acknowledgments—Support for the Comprehensive Flow Cytometry Core provided by National Institutes of Health P30AR048311 and National Institutes of Health P30AI27667.

Author contributions—J. L. L.-C. and A. B. C. conceptualization; J. L. L.-C., L. G., J. K., and A. D. data curation; J. L. L.-C. and L. G. formal analysis; J. L. L.-C., L. G., J. K., A. B. C., and A. D. investigation; J. L. L.-C. and A. B. C. methodology; J. L. L.-C. and A. B. C. writing-original draft; J. L. L.-C, L. G., and A. B. C. resources; A. B. C. supervision; A. B. C. funding acquisition; A. B. C. validation; A. B. C. project administration; A. B. C. writing-review and editing.

Funding and additional information—Research reported in this publication was supported by the National Institutes of Health grants 2R01 ES015981-13 and P42 ES027723-2 and Department of Veteran Affairs Merit Review 1 I01 CX001715-2 to A. B. C. The content is solely the responsibility of the authors and does not necessarily represent the official views of the National Institutes of Health.

Conflict of interest—The authors declare that they have no conflicts of interest with the contents of this article.

Abbreviations—The abbreviations used are: AEC, alveolar epithelial cell; ASK1, apoptosis signal-regulating kinase 1; BAD, Bcl-2-associated death; BMDM, bone-marrow-derived macrophage; Csf1r, colony-stimulating factor 1 receptor; IPF, idiopathic pulmonary fibrosis; MDM, monocyte-derived macrophage; MMVF, man-made vitreous fiber; NOX4, NADPH oxidase 4; PKB, protein kinase

B; RAM, resident alveolar macrophage; ROS, reactive oxygen species.

References

1. Attfield, M. D., Wood, J. M., Antao, V. C., and Pinheiro, G. A. (2004) Changing patterns of pneumoconiosis mortality–United States, 1968-2000. *MMWR Morb. Mortal Wkly. Rep.* **53**, 627–632
2. Guidotti, T. L., Miller, A., Christiani, D., Wagner, G., Balmes, J., Harber, P., Brodkin, C. A., Rom, W., Hillerdal, G., Harbut, M., and Green, F. H. Y. (2004) Diagnosis and initial management of nonmalignant diseases related to asbestos. *Am. J. Respir. Crit. Care Med.* **170**, 691–715
3. Yang, M., Wang, D., Gan, S., Fan, L., Cheng, M., Yu, L., Wang, B., Li, W., Ma, J., Zhou, M., and Chen, W. (2020) Increasing incidence of asbestosis worldwide, 1990-2017: Results from the Global Burden of Disease study 2017. *Thorax* **75**, 798–800
4. King, T. E., Jr., Bradford, W. Z., Castro-Bernardini, S., Fagan, E. A., Glaspole, I., Glassberg, M. K., Gorina, E., Hopkins, P. M., Kardatzke, D., Lancaster, L., Lederer, D. J., Nathan, S. D., Pereira, C. A., Sahn, S. A., Sussman, R., *et al.* (2014) A phase 3 trial of pirfenidone in patients with idiopathic pulmonary fibrosis. *N. Engl. J. Med.* **370**, 2083–2092
5. Richeldi, L., du Bois, R. M., Raghu, G., Azuma, A., Brown, K. K., Costabel, U., Cottin, V., Flaherty, K. R., Hansell, D. M., Inoue, Y., Kim, D. S., Kolb, M., Nicholson, A. G., Noble, P. W., Selman, M., *et al.* (2014) Efficacy and safety of nintedanib in idiopathic pulmonary fibrosis. *N. Engl. J. Med.* **370**, 2071–2082
6. Murthy, S., Ryan, A., He, C., Mallampalli, R. K., and Carter, A. B. (2010) Rac1-mediated mitochondrial H2O2 generation regulates MMP-9 gene expression in macrophages via inhibition of SP-1 and AP-1. *J. Biol. Chem.* **285**, 25062–25073
7. Osborn-Heaford, H. L., Ryan, A. J., Murthy, S., Racila, A. M., He, C., Sieren, J. C., Spitz, D. R., and Carter, A. B. (2012) Mitochondrial Rac1 GTPase import and electron transfer from cytochrome c are required for pulmonary fibrosis. *J. Biol. Chem.* **287**, 3301–3312
8. He, C., Murthy, S., McCormick, M. L., Spitz, D. R., Ryan, A. J., and Carter, A. B. (2011) Mitochondrial Cu,Zn-Superoxide Dismutase mediates pulmonary fibrosis by augmenting H2O2 generation. *J. Biol. Chem.* **286**, 15597–15607
9. Misharin, A. V., Morales-Nebreda, L., Reyfman, P. A., Cuda, C. M., Walter, J. M., McQuattie-Pimentel, A. C., Chen, C. I., Anekalla, K. R., Joshi, N., Williams, K. J. N., Abdala-Valencia, H., Yacoub, T. J., Chi, M., Chiu, S., Gonzalez-Gonzalez, F. J., *et al.* (2017) Monocyte-derived alveolar macrophages drive lung fibrosis and persist in the lung over the life span. *J. Exp. Med.* **214**, 2387–2404
10. McCubbrey, A. L., Barthel, L., Mohning, M. P., Redente, E. F., Mould, K. J., Thomas, S. M., Leach, S. M., Danhorn, T., Gibbings, S. L., Jakubzick, C. V., Henson, P. M., and Janssen, W. J. (2018) Deletion of c-FLIP from CD11b(hi) macrophages prevents development of bleomycin-induced lung fibrosis. *Am. J. Respir. Cell Mol. Biol.* **58**, 66–78
11. He, C., Larson-Casey, J. L., Davis, D., Hanumanthu, V. S., Longhini, A. L. F., Thannickal, V. J., Gu, L., and Carter, A. B. (2019) NOX4 modulates macrophage phenotype and mitochondrial biogenesis in asbestosis. *JCI Insight* **4**
12. Larson-Casey, J. L., Vaid, M., Gu, L., He, C., Cai, G. Q., Ding, Q., Davis, D., Berryhill, T. F., Wilson, L. S., Barnes, S., Neighbors, J. D., Hohl, R. J., Zimmerman, K. A., Yoder, B. K., Longhini, A. L. F., *et al.* (2019) Increased flux through the mevalonate pathway mediates fibrotic repair without injury. *J. Clin. Invest.* **129**, 4962–4978
13. Gu, L., Larson Casey, J. L., Andrabi, S. A., Lee, J. H., Meza-Perez, S., Randall, T. D., and Carter, A. B. (2019) Mitochondrial calcium uniporter regulates PGC-1alpha expression to mediate metabolic reprogramming in pulmonary fibrosis. *Redox Biol.* **26**, 101307
14. He, C., Ryan, A. J., Murthy, S., and Carter, A. B. (2013) Accelerated development of pulmonary fibrosis via Cu,Zn-superoxide dismutase-induced alternative activation of macrophages. *J. Biol. Chem.* **288**, 20745–20757
15. Murthy, S., Larson-Casey, J. L., Ryan, A. J., He, C., Kobzik, L., and Carter, A. B. (2015) Alternative activation of macrophages and pulmonary fibrosis are modulated by scavenger receptor, macrophage receptor with collagenous structure. *FASEB J.* **29**, 3527–3536
16. Redente, E. F., Keith, R. C., Janssen, W., Henson, P. M., Ortiz, L. A., Downey, G. P., Bratton, D. L., and Riches, D. W. (2014) Tumor necrosis factor-alpha accelerates the resolution of established pulmonary fibrosis in mice by targeting profibrotic lung macrophages. *Am. J. Respir. Cell Mol. Biol.* **50**, 825–837
17. Larson-Casey, J. L., Deshane, J. S., Ryan, A. J., Thannickal, V. J., and Carter, A. B. (2016) Macrophage Akt1 kinase-mediated mitophagy modulates apoptosis resistance and pulmonary fibrosis. *Immunity* **44**, 582–596
18. Plataki, M., Koutsopoulos, A. V., Darivianaki, K., Delides, G., Siafakas, N. M., and Bouros, D. (2005) Expression of apoptotic and antiapoptotic markers in epithelial cells in idiopathic pulmonary fibrosis. *Chest* **127**, 266–274
19. Hecker, L., Logsdon, N. J., Kurundkar, D., Kurundkar, A., Bernard, K., Hock, T., Meldrum, E., Sanders, Y. Y., and Thannickal, V. J. (2014) Reversal of persistent fibrosis in aging by targeting Nox4-Nrf2 redox imbalance. *Sci. Transl. Med.* **6**, 231ra247
20. Nisimoto, Y., Diebold, B. A., Cosentino-Gomes, D., and Lambeth, J. D. (2014) Nox4: A hydrogen peroxide-generating oxygen sensor. *Biochemistry* **53**, 5111–5120
21. Carnesecchi, S., Deffert, C., Donati, Y., Basset, O., Hinz, B., Preynat-Seauve, O., Guichard, C., Arbiser, J. L., Banfi, B., Pache, J. C., Barazzone-Argiroffo, C., and Krause, K. H. (2011) A key role for NOX4 in epithelial cell death during development of lung fibrosis. *Antioxid. Redox Signal* **15**, 607–619
22. Bernard, K., Logsdon, N. J., Miguel, V., Benavides, G. A., Zhang, J., Carter, A. B., Darley-Usmar, V. M., and Thannickal, V. J. (2017) NADPH oxidase 4 (Nox4) suppresses mitochondrial biogenesis and bioenergetics in lung fibroblasts via a nuclear factor erythroid-derived 2-like 2 (Nrf2)-dependent pathway. *J. Biol. Chem.* **292**, 3029–3038
23. Larson-Casey, J. L., Murthy, S., Ryan, A. J., and Carter, A. B. (2014) Modulation of the mevalonate pathway by Akt regulates macrophage survival and development of pulmonary fibrosis. *J. Biol. Chem.* **289**, 36204–36219
24. Spadoni, T., Svegliati Baroni, S., Amico, D., Albani, L., Moroncini, G., Avvedimento, E. V., and Gabrielli, A. (2015) A reactive oxygen species-mediated loop maintains increased expression of NADPH oxidases 2 and 4 in skin fibroblasts from patients with systemic sclerosis. *Arthritis Rheumatol.* **67**, 1611–1622
25. Sancho, P., Mainez, J., Crosas-Molist, E., Roncero, C., Fernandez-Rodriguez, C. M., Pinedo, F., Huber, H., Eferl, R., Mikulits, W., and Fabregat, I. (2012) NADPH oxidase NOX4 mediates stellate cell activation and hepatocyte cell death during liver fibrosis development. *PLoS One* **7**, e45285
26. Masamune, A., Watanabe, T., Kikuta, K., Satoh, K., and Shimosegawa, T. (2008) NADPH oxidase plays a crucial role in the activation of pancreatic stellate cells. *Am. J. Physiol. Gastrointest. Liver Physiol.* **294**, G99–G108
27. Sedeek, M., Callera, G., Montezano, A., Gutsol, A., Heitz, F., Szyndralewiez, C., Page, P., Kennedy, C. R., Burns, K. D., Touyz, R. M., and Hebert, R. L. (2010) Critical role of Nox4-based NADPH oxidase in glucose-induced oxidative stress in the kidney: Implications in type 2 diabetic nephropathy. *Am. J. Physiol. Renal Physiol.* **299**, F1348–F1358
28. Cucoranu, I., Clempus, R., Dikalova, A., Phelan, P. J., Ariyan, S., Dikalov, S., and Sorescu, D. (2005) NAD(P)H oxidase 4 mediates transforming growth factor-beta1-induced differentiation of cardiac fibroblasts into myofibroblasts. *Circ. Res.* **97**, 900–907
29. Hecker, L., Vittal, R., Jones, T., Jagirdar, R., Luckhardt, T. R., Horowitz, J. C., Pennathur, S., Martinez, F. J., and Thannickal, V. J. (2009) NADPH oxidase-4 mediates myofibroblast activation and fibrogenic responses to lung injury. *Nat. Med.* **15**, 1077–1081
30. Hagimoto, N., Kuwano, K., Miyazaki, H., Kunitake, R., Fujita, M., Kawasaki, M., Kaneko, Y., and Hara, N. (1997) Induction of apoptosis and pulmonary fibrosis in mice in response to ligation of Fas antigen. *Am. J. Respir. Cell Mol. Biol.* **17**, 272–278
31. Lawson, W. E., Cheng, D. S., Degryse, A. L., Tanjore, H., Polosukhin, V. V., Xu, X. C., Newcomb, D. C., Jones, B. R., Roldan, J., Lane, K. B., Morrisey, E. E., Beers, M. F., Yull, F. E., and Blackwell, T. S. (2011)

Endoplasmic reticulum stress enhances fibrotic remodeling in the lungs. *Proc. Natl. Acad. Sci. U. S. A.* **108**, 10562–10567
32. Zhou, Y., Huang, X., Hecker, L., Kurundkar, D., Kurundkar, A., Liu, H., Jin, T. H., Desai, L., Bernard, K., and Thannickal, V. J. (2013) Inhibition of mechanosensitive signaling in myofibroblasts ameliorates experimental pulmonary fibrosis. *J. Clin. Invest.* **123**, 1096–1108
33. Tanaka, T., Yoshimi, M., Maeyama, T., Hagimoto, N., Kuwano, K., and Hara, N. (2002) Resistance to Fas-mediated apoptosis in human lung fibroblast. *Eur. Respir. J.* **20**, 359–368
34. Hamilton, R. F., Jr., Li, L., Felder, T. B., and Holian, A. (1995) Bleomycin induces apoptosis in human alveolar macrophages. *Am. J. Physiol.* **269**, L318–L325
35. Wang, L., Scabilloni, J. F., Antonini, J. M., Rojanasakul, Y., Castranova, V., and Mercer, R. R. (2006) Induction of secondary apoptosis, inflammation, and lung fibrosis after intratracheal instillation of apoptotic cells in rats. *Am. J. Physiol. Lung Cell Mol. Physiol.* **290**, L695–L702
36. Jacobsen, K., Bertran-Alamillo, J., Molina, M. A., Teixido, C., Karachaliou, N., Pedersen, M. H., Castellvi, J., Garzon, M., Codony-Servat, C., Codony-Servat, J., Gimenez-Capitan, A., Drozdowskyj, A., Viteri, S., Larsen, M. R., Lassen, U., *et al.* (2017) Convergent Akt activation drives acquired EGFR inhibitor resistance in lung cancer. *Nat. Commun.* **8**, 410
37. Yan, F., Wang, Y., Wu, X., Peshavariya, H. M., Dusting, G. J., Zhang, M., and Jiang, F. (2014) Nox4 and redox signaling mediate TGF-beta-induced endothelial cell apoptosis and phenotypic switch. *Cell Death Dis.* **5**, e1010
38. Zhao, Q. D., Viswanadhapalli, S., Williams, P., Shi, Q., Tan, C., Yi, X., Bhandari, B., and Abboud, H. E. (2015) NADPH oxidase 4 induces cardiac fibrosis and hypertrophy through activating Akt/mTOR and NFkappaB signaling pathways. *Circulation* **131**, 643–655
39. Gorin, Y., Ricono, J. M., Kim, N. H., Bhandari, B., Choudhury, G. G., and Abboud, H. E. (2003) Nox4 mediates angiotensin II-induced activation of Akt/protein kinase B in mesangial cells. *Am. J. Physiol. Renal Physiol.* **285**, F219–F229
40. Palmieri, M., Pal, R., Nelvagal, H. R., Lotfi, P., Stinnett, G. R., Seymour, M. L., Chaudhury, A., Bajaj, L., Bondar, V. V., Bremner, L., Saleem, U., Tse, D. Y., Sanagasetti, D., Wu, S. M., Neilson, J. R., *et al.* (2017) mTORC1-independent TFEB activation via Akt inhibition promotes cellular clearance in neurodegenerative storage diseases. *Nat. Commun.* **8**, 14338
41. Cho, H., Mu, J., Kim, J. K., Thorvaldsen, J. L., Chu, Q., Crenshaw, E. B., 3rd, Kaestner, K. H., Bartolomei, M. S., Shulman, G. I., and Birnbaum, M. J. (2001) Insulin resistance and a diabetes mellitus-like syndrome in mice lacking the protein kinase Akt2 (PKB beta). *Science* **292**, 1728–1731
42. Campa, C. C., Silva, R. L., Margaria, J. P., Pirali, T., Mattos, M. S., Kraemer, L. R., Reis, D. C., Grosa, G., Copperi, F., Dalmarco, E. M., Lima-Junior, R. C. P., Aprile, S., Sala, V., Dal Bello, F., Prado, D. S., *et al.* (2018) Inhalation of the prodrug PI3K inhibitor CL27c improves lung function in asthma and fibrosis. *Nat. Commun.* **9**, 5232
43. Xu, Y., Mizuno, T., Sridharan, A., Du, Y., Guo, M., Tang, J., Wikenheiser-Brokamp, K. A., Perl, A. T., Funari, V. A., Gokey, J. J., Stripp, B. R., and Whitsett, J. A. (2016) Single-cell RNA sequencing identifies diverse roles of epithelial cells in idiopathic pulmonary fibrosis. *JCI Insight* **1**, e90558
44. Xia, H., Diebold, D., Nho, R., Perlman, D., Kleidon, J., Kahm, J., Avdulov, S., Peterson, M., Nerva, J., Bitterman, P., and Henke, C. (2008) Pathological integrin signaling enhances proliferation of primary lung fibroblasts from patients with idiopathic pulmonary fibrosis. *J. Exp. Med.* **205**, 1659–1672
45. Yang, E., Zha, J., Jockel, J., Boise, L. H., Thompson, C. B., and Korsmeyer, S. J. (1995) Bad, a heterodimeric partner for Bcl-XL and Bcl-2, displaces Bax and promotes cell death. *Cell* **80**, 285–291
46. Datta, S. R., Dudek, H., Tao, X., Masters, S., Fu, H., Gotoh, Y., and Greenberg, M. E. (1997) Akt phosphorylation of BAD couples survival signals to the cell-intrinsic death machinery. *Cell* **91**, 231–241
47. von Harsdorf, R., Li, P. F., and Dietz, R. (1999) Signaling pathways in reactive oxygen species-induced cardiomyocyte apoptosis. *Circulation* **99**, 2934–2941